Article

Probing Local Structure in Zeolite Frameworks: Ultrahigh-Field NMR Measurements and Accurate First-Principles Calculations of Zeolite Si Magnetic Shielding Tensors

Darren H. Brouwer, and Gary D. Enright

J. Am. Chem. Soc., **2008**, 130 (10), 3095-3105 • DOI: 10.1021/ja077430a

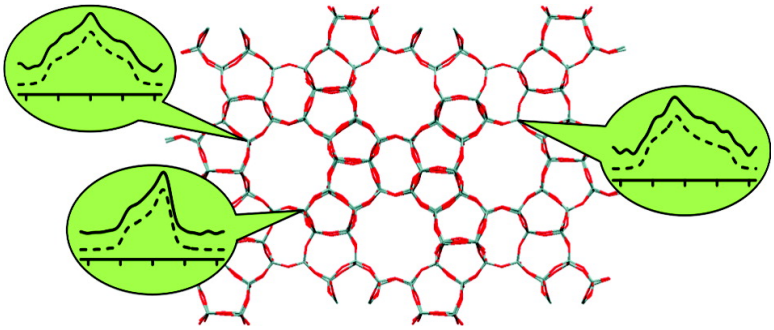

J|A|C|S
ARTICLES
Published on Web 02/19/2008

Probing Local Structure in Zeolite Frameworks: Ultrahigh-Field NMR Measurements and Accurate First-Principles Calculations of Zeolite ^{29}Si Magnetic Shielding Tensors

Darren H. Brouwer* and Gary D. Enright

Steacie Institute for Molecular Sciences, National Research Council, 100 Sussex Drive, Ottawa, Ontario K1A 0R6, Canada

Received October 2, 2007; E-mail: Darren.Brouwer@nrc-cnrc.gc.ca

Abstract: The principal components of zeolite ^{29}Si magnetic shielding tensors have been accurately measured *and* calculated for the first time. The experiments were performed at an ultrahigh magnetic field of 21.1 T in order to observe the small anisotropies of the ^{29}Si shielding interactions that arise for Si atoms in near-tetrahedral geometries. A robust two-dimensional (2D) chemical shift anisotropy (CSA) recoupling pulse sequence was employed that enables quasi-static powder patterns to be resolved according to the isotropic chemical shifts. For the zeolites Sigma-2 and ZSM-12, it is demonstrated that the ^{29}Si chemical shift (CS) tensor components measured by the recoupling experiment are in excellent agreement with those determined from spinning sidebands in slow magic-angle spinning (MAS) experiments. For the zeolite ZSM-5, the principal components of the ^{29}Si CS tensors of 15 of the 24 Si sites were measured using the 2D CSA recoupling experiment, a feat that would not be possible with a slow MAS experiment due to the complexity of the spectrum. A simple empirical relationship between the ^{29}Si CS tensors and local structural parameters could not be established. However, the ^{29}Si magnetic shielding tensors calculated using Hartree−Fock *ab initio* calculations on clusters derived from the crystal structures are in excellent agreement with the experimental results. The accuracy of the calculations is strongly dependent on the quality of the crystal structure used in the calculation, indicating that the ^{29}Si magnetic shielding interaction is extremely sensitive to the local structure around each Si atom. It is anticipated that the measurement and calculation of ^{29}Si shielding tensors could be incorporated into the "NMR crystallography" of zeolites and other related silicate materials, possibly being used for structure refinements that may lead to crystal structures with very accurate Si and O atomic coordinates.

Introduction

The integration of complementary structural characterization techniques is a powerful strategy that often leads to a better understanding of the structure and dynamics of many important solid materials including zeolites, inclusion compounds, biomolecules, and pharmaceuticals. In particular, the combination of experimental solid-state NMR and X-ray diffraction (XRD) methods with computer modeling and quantum chemical calculations forms a powerful approach that is being used more and more by structural chemists for the characterization of increasingly complex materials, particularly for those materials that are difficult to obtain as large single crystals. The recent successes of solid-state NMR spectroscopy in determining the structures of various materials[1−9] has led to the emergence of the term "NMR crystallography", which broadly refers to the incorporation of solid-state NMR data in varying degrees in the structure determination of materials, usually in combination with XRD and computational methods.

Solid-state NMR can provide valuable information for the various stages in the determination of a crystal structure. The number of peaks and their relative intensities reflect the number and occupancies of unique crystallographic sites in the structure and may be used to identify possible space groups.[10−12] Information about connectivities or distances between atoms, in the form of *J*-couplings or dipolar couplings between nuclei, can be used to constrain or build structural models.[1−5,13] Chemical shift and quadrupolar parameters provide very sensi-

(1) Brouwer, D. H.; Darton, R. J.; Morris, R. E.; Levitt, M. H. *J. Am. Chem. Soc.* **2005**, *127*, 10365.
(2) Fyfe, C. A.; Brouwer, D. H. *J. Am. Chem. Soc.* **2006**, *128*, 11860.
(3) Dutour, J.; Guillou, N.; Huguenard, C.; Taulelle, F.; Mellot-Draznieks, C.; Ferey, G. *Solid State Sci.* **2004**, *6*, 1059.
(4) Hedin, N.; Graf, R.; Christiansen, S. C.; Gervais, C.; Hayward, R. C.; Eckert, J.; Chmelka, B. F. *J. Am. Chem. Soc.* **2004**, *126*, 9425.
(5) Elena, B.; Pintacuda, G.; Mifsud, N.; Emsley, L. *J. Am. Chem. Soc.* **2006**, *128*, 9555.
(6) Pickard, C. J.; Salager, E.; Pintacuda, G.; Elena, B.; Emsley, L. *J. Am. Chem. Soc.* **2007**, *129*, 8932.
(7) Castellani, F.; van Rossum, B.; Diehl, A.; Schubert, M.; Rehbien, K.; Oschkinat, H. *Nature* **2002**, *420*, 98.
(8) Zech, S. G.; Wand, A. J.; McDermott, A. E. *J. Am. Chem. Soc.* **2005**, *127*, 8618.
(9) Baldus, M. *Angew. Chem., Int. Ed.* **2006**, *45*, 1186.
(10) Fyfe, C. A.; Gies, H.; Kokotailo, G. T.; Marler, B.; Cox, D. E. *J. Phys. Chem.* **1990**, *94*, 3718.
(11) King, I. J.; Fayon, F.; Massiot, D.; Harris, R. K.; Evans, J. S. O. *Chem. Commun.* **2001**, 1766.
(12) Taulelle, F. *Solid State Sci.* **2004**, *6*, 1053.
(13) Fyfe, C. A.; Diaz, A. C.; Grondey, H.; Lewis, A. R.; Forster, H. *J. Am. Chem. Soc.* **2005**, *127*, 7543.

tive information about local structural environments and can be used to test structural models[6,14−16] or to potentially refine structures when used in combination with *ab initio* calculations. The focus of this paper is the development of NMR crystallography tools and strategies that incorporate chemical shift information into the structure determination of materials, particularly at the structure refinement stage.

The application of NMR crystallography to pure silica zeolites has been particularly successful.[1,2,13,17] Zeolites are very important materials, with their properties intimately connected to their three-dimensional architectures, yet their structural characterization is not straightforward due to the complexity of the structures and the fact that single crystals cannot usually be obtained. It has been demonstrated that zeolite crystal structures can be determined by a combination of ^{29}Si NMR and powder XRD, with the crucial step of structure solution being achieved from advanced ^{29}Si double-quantum NMR experiments.[1,17] The structures are solved in the sense that the three-dimensional topologies, as defined by the positions and connectivities of the Si atoms, of the zeolite structure are established. This, however, does not provide the complete structure. The positions of the bridging oxygen atoms remain unknown, although to a first approximation it can be assumed that they fall somewhere between connected Si atoms. It is anticipated that the ^{29}Si chemical shift (CS) tensors could reveal very detailed structural information about the local geometries around each Si site and therefore be used to provide a more accurate and complete picture of zeolite crystal structures. However, before this can be done, two major obstacles have to be overcome. First, the measurement of zeolite ^{29}Si CS tensors is not usually straightforward. Second, a reliable relationship between local structural geometry and the measured ^{29}Si CS tensor parameters must be established.

There are two major challenges in measuring zeolite ^{29}Si CS tensors that have prevented their measurement until this point. First, the Si atoms in pure silica zeolites are located in Q^4 coordination environments that are close to ideal tetrahedral symmetry (Q^n denotes a silicon site in tetrahedral coordination with four O atoms in the first coordination sphere and n Si atoms in the second). Consequently, there is only a weak dependence of the magnetic shielding interaction on the orientation with respect to the magnetic field, leading to chemical shift anisotropies that are presumed to be quite small. For example, the span of the ^{29}Si shielding tensor in α-quartz has been estimated to be 6.5 ppm.[18] With the recent availability of ultrahigh-field NMR instruments, it is possible to take advantage of the fact that the shielding interaction (in hertz) scales with magnetic field strength. Second, the ^{29}Si NMR spectra of zeolites tend to be quite complex, with many resolved isotropic peaks arising from the unique Si sites in the crystal structures, making it difficult, if not impossible, to collect ^{29}Si magic-angle spinning (MAS) NMR spectra with spinning sideband patterns whose peaks do not overlap with one another. Advances in NMR pulse sequence design have given rise to "recoupling" experiments in which MAS provides the required spectral resolution while carefully timed pulses selectively reintroduce a particular nuclear spin interaction, such as the chemical shift anisotropy (CSA), and observe it indirectly in a second dimension.

The measurement of zeolite ^{29}Si CS tensors has not been previously reported, and only a limited number of ^{29}Si CS tensor measurements have been reported for related silicate materials. Various ^{29}Si static and MAS NMR experiments have been performed for natural and synthetic silicate minerals.[19−22] However in these materials, the Si atoms were located in Q^0 to Q^3 coordination environments, for which there exists a significant degree of anisotropy of the shielding tensors, making the measurements relatively straightforward. ^{29}Si CS tensor components for Q^4 sites in silyl silicate cage materials have been obtained from spinning sideband patterns in ^{29}Si MAS NMR spectra.[23] A single-crystal ^{29}Si NMR study has been performed on α-quartz from which both the orientation and principal components of the ^{29}Si CS tensor were estimated.[18] Multiple-pulse two-dimensional (2D) ^{29}Si CSA recoupling and magic-angle turning experiments have been reported previously for the crystalline silicate mineral Wollastanite,[24] disordered silicate glasses,[24,25] and a layered silicate material.[4] Again, the principal components of the ^{29}Si CS tensors for Q^3 sites in the crystalline materials were easily measured, but the information obtained for Q^4 sites is very limited.

The second challenge is to establish a relationship between ^{29}Si CS tensors and the local structure of the Si sites in zeolite frameworks. Semiempirical relationships between ^{29}Si isotropic chemical shifts and local structural geometry for pure silica zeolites have been established,[26−34] and this work has been reviewed by Mackenzie and Smith.[35] Changes in the Si−O−Si bond angle lead to changes in the degree of s and p orbital hybridization on the bridging oxygen atoms, which in turn lead to changes in oxygen orbital electronegativities and different paramagnetic contributions to magnetic shielding of the ^{29}Si nuclei.[28] The degree of s character of the oxygen bond orbital is given by $\rho = \cos\alpha/(\cos\alpha - 1)$, where α is the Si−O−Si bond angle.[36] It has been demonstrated that there exists a linear relationship between ^{29}Si isotropic chemical shift and the mean oxygen s character, $\bar{\rho}$, of the oxygen atoms around each Si atom.[28,32] It is not obvious, however, what sort of relationship

(14) Harper, J. K.; Grant, D. M. *Cryst. Growth Des.* **2006**, *6*, 2315.
(15) Harper, J. K.; Grant, D. M.; Zhang, Y.; Lee, P. L.; Von Dreele, R. *J. Am. Chem. Soc.* **2006**, *128*, 1547.
(16) Harris, R. K. *Solid State Sci.* **2004**, *6*, 1025.
(17) Brouwer, D. H.; Kristiansen, P. E.; Fyfe, C. A.; Levitt, M. H. *J. Am. Chem. Soc.* **2005**, *127*, 542.
(18) Spearing, D. R.; Stebbins, J. F. *Am. Mineral.* **1989**, *74*, 956.
(19) Grimmer, A. R.; Peter, R.; Fechner, E.; Molgedey, G. *Chem. Phys. Lett.* **1981**, *77*, 331.
(20) Smith, K. A.; Kirkpatrick, R. J.; Oldfield, E.; Henderson, D. M. *Am. Mineral.* **1983**, *68*, 1206.
(21) Matijasic, A.; Lewis, A. R.; Marichal, C.; Delmotte, L.; Chezeau, J. M.; Patarin, J. *Phys. Chem. Chem. Phys.* **2000**, *2*, 2807.
(22) Hansen, M. R.; Jakobsen, H. J.; Skibsted, J. *Inorg. Chem.* **2003**, *42*, 2368.
(23) Backer, M.; Grimmer, A. R.; Auner, N.; John, P.; Weis, J. *Solid State Nucl. Magn. Reson.* **1997**, *9*, 241.
(24) Sakellariou, D.; Jacquinot, J.-F.; Charpentier, T. *Chem. Phys. Lett.* **2005**, *411*, 171.
(25) Duer, M. J.; Elliott, S. R.; Gladden, L. F. *J. Non-Cryst. Solids* **1995**, *189*, 107.
(26) Smith, J. V.; Blackwell, C. S. *Nature* **1983**, *303*, 223.
(27) Thomas, J. M.; Klinowski, J.; Ramdas, S.; Hunter, B. K.; Tennakoon, D. T. B. *Chem. Phys. Lett.* **1983**, *102*, 158.
(28) Engelhardt, G.; Radeglia, R. *Chem. Phys. Lett.* **1984**, *108*, 271.
(29) Groenen, E. J. J.; Alma, N. C. M.; Dorrepaal, J.; Hays, G. R.; Kortbeek, A. G. T. G. *Zeolites* **1985**, *5*, 361.
(30) Fyfe, C. A.; Strobl, H.; Kokotailo, G. T.; Pasztor, C. T.; Barlow, G. E.; Bradley, S. *Zeolites* **1988**, *8*, 132.
(31) Sherriff, B.; Grundey, H. D.; Hartman, J. S. *Eur. J. Mineral.* **1991**, *3*, 751.
(32) Fyfe, C. A.; Feng, Y.; Grondey, H. *Microporous Mater.* **1993**, *1*, 393.
(33) Hochgrafe, M.; Gies, H.; Fyfe, C. A.; Feng, Y.; Grondey, H. *Chem. Mater.* **2000**, *12*, 336.
(34) Sivadinarayana, C.; Choudhary, V. R.; Vetrivel, R.; Ganapathy, S. *Solid State Nucl. Magn. Reson.* **1998**, *13*, 175.
(35) Mackenzie, K. J. D.; Smith, M. E. *Multinuclear Solid-State NMR of Inorganic Materials*; Pergamon Press: Oxford, 2002; Chapter 4.
(36) Gibbs, G. V. *Am. Mineral.* **1982**, *67*, 421.

would exist between the local structural geometry and the components of the ^{29}Si CS tensors. *Ab initio* calculations provide a method to explore such a relationship, particularly if it can be demonstrated that ^{29}Si shielding tensors can be accurately calculated from a known crystal structure.

Previous reports of *ab initio* calculations of ^{29}Si NMR parameters in zeolites and silica polymorphs are restricted to calculations of isotropic shifts.[37−46] Most of the papers describe calculations of the ^{29}Si isotropic values using cluster models extracted from the crystal structures for silica polymorphs,[37,38] possible zeolite precursors,[39] and a number of different zeolites.[40−44] Periodic density functional theory (DFT) calculations of ^{29}Si and ^{17}O isotropic shifts and ^{17}O quadrupolar parameters using the full unit cells of crystal structures have been reported for a number of silica polymorphs, including the zeolites ferrierite and faujasite.[45] Most of these calculations demonstrate good agreement with experimental ^{29}Si isotropic chemical shifts, suggesting that it may be possible to accurately calculate the components of the ^{29}Si shielding tensors as well.

It is demonstrated here, for the first time, that the principal components of ^{29}Si CS tensors can be measured in zeolite powders. A 2D CSA recoupling sequence is employed in which the anisotropy of the CS tensor is reintroduced by applying a series of rotor-synchronized pulses and correlated to the isotropic chemical shifts. The experiments were carried out at an ultrahigh-field NMR facility (21.1 T), which dramatically improves the reliability of the measurements. In addition, it is demonstrated that the principal components of zeolite ^{29}Si shielding tensors can indeed be accurately calculated with Hartree−Fock *ab initio* calculations on clusters extracted from zeolite crystal structures. The quality of agreement with experimental data is very sensitive to the quality of the crystal structure used for the calculations, demonstrating that ^{29}Si CS tensors are a very sensitive probe of the local structural environment in zeolite frameworks.

Experimental Section

Syntheses of the samples used in this work (Sigma-2,[47] silica-ZSM-12,[10] and silica-ZSM-5[48]) have been described previously.

Solid-state NMR experiments were carried out on a Bruker AVANCE-II 900 MHz NMR spectrometer operating at a magnetic field of 21.1 T (178.831 MHz ^{29}Si Larmor frequency) using a standard-bore double-resonance 4 mm MAS NMR probe. The samples were confined to the middle one-third of the MAS rotors in order to minimize the effects of radiofrequency (rf) inhomogeneity. The ^{29}Si chemical shifts were referenced by setting the ^{29}Si resonance for a sample of neat liquid tetramethylsilane (TMS) sealed in a 3 mm glass tube to 0 ppm.

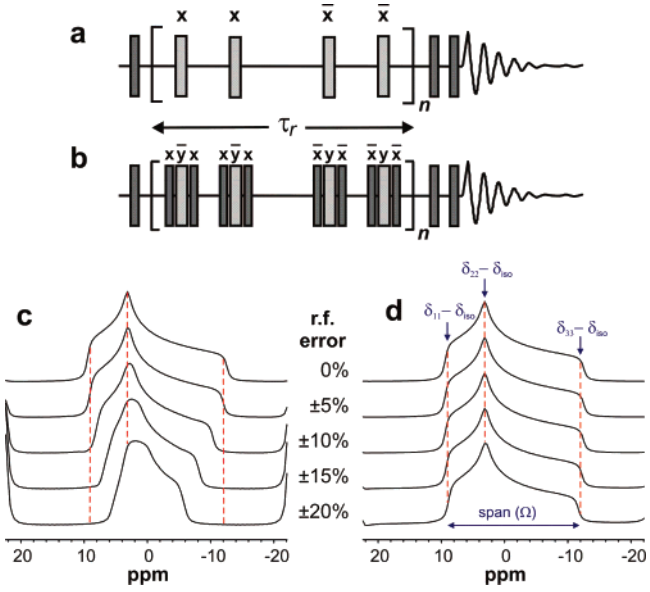

Figure 1. (a,b) Pulse sequence diagrams for CSA recoupling pulse sequences with (a) regular or (b) composite 180° recoupling pulses. The dark and light shaded boxes represent 90° and 180° pulses, respectively. (c,d) Simulated CSA recoupled quasi-static line shapes (Ω = 21 ppm and κ = 0.43) as functions of the error in rf amplitude in (c) regular 180° recoupling pulses and (d) composite 180° recoupling pulses.

A modified version of the 2D 4 π-pulse CSA recoupling sequence introduced by Tycko et al.[49] was used in this work (Figure 1b). The sequence correlates quasi-static powder line shapes to the isotropic chemical shifts. These quasi-static powder line shapes have the same shape as static powder line shapes but are narrowed by a scaling factor of 0.393 and have their centers of gravity at zero frequency in the indirect dimension. Due to the sensitivity of the CSA recoupled line shapes to errors in the rf amplitude of the 180° recoupling pulses (Figure 1c), composite 180° pulses were used instead, which dramatically decreases the sensitivity to rf amplitude error (Figure 1d). Further details about the implementation of the pulse sequence can be found in the Supporting Information.

The pulse sequence was implemented with ^{29}Si 90° and 180° pulses of 3.2 and 6.4 μs, respectively. The experiments for Sigma-2 were carried out at a spinning frequency of 2500 Hz and employed 20 ms of cross polarization from the protons of the template molecule, a recycle delay of 2 s, and a proton-decoupling rf field of approximately 80 kHz during the CSA recoupling period but no proton decoupling during the acquisition period. A total of 16 t_1 increments, each with two spectra, were acquired with 32 scans. The experiments for the zeolite samples were carried out at 3000 Hz and did not employ cross polarization or decoupling. The experiment for ZSM-12 employed a recycle delay of 15 s and 16 t_1 increments with 96 scans. The experiment for the monoclinic phase of silica-ZSM-5 employed a recycle delay of 15 s and 12 t_1 increments with 704 scans.

Simulations and fitting were carried out using the SIMPSON simulation program[50] in order to estimate ^{29}Si CS tensor values from the experimental spectra. In all simulations, powder averaging was carried out using 986 pairs of α and β angles selected according to the ZCW method[51−53] and 100 γ angles. The Herzfeld−Berger convention[54]

(37) Mauri, F.; Pasquarello, A.; Pfrommer, B. G.; Yoon, Y.-G.; Louie, S. G. *Phys. Rev. B* **2000**, *62*, R4786.
(38) Xue, X.; Kanzaki, M. *Solid State Nucl. Magn. Reson.* **2000**, *16*, 245.
(39) Azizi, S. N.; Rostami, A. A.; Godarzia, A. A. *J. Phys. Soc. Jpn.* **2005**, *74*, 1609.
(40) Bull, L. M.; Bussemer, B.; Anupold, T.; Reinhold, A.; Samoson, A.; Sauer, J.; Cheetham, A. K.; Dupree, R. *J. Am. Chem. Soc.* **2000**, *122*, 4948.
(41) Bussemer, B.; Schroder, K.-P.; Sauer, J. *Solid State Nucl. Magn. Reson.* **1997**, *9*, 155.
(42) Valerio, G.; Goursot, A.; Vetrivel, R.; Malkina, O.; Malkin, V.; Salahub, D. R. *J. Am. Chem. Soc.* **1998**, *120*, 11426.
(43) Valerio, G.; Goursot, A.; Vetrivel, R.; Salahub, D. R. *Microporous Mesoporous Mater.* **1999**, *30*, 111.
(44) Wolff, R.; Jancke, H.; Radeglia, R. *Solid State Nucl. Magn. Reson.* **1997**, *9*, 177.
(45) Profeta, M.; Mauri, F.; Pickard, C. J. *J. Am. Chem. Soc.* **2003**, *125*, 541.
(46) Goursot, A.; Berthomieu, D. In *Calculation of NMR and EPR Parameters: Theory and Applications*; Kaupp, M., Bühl, M., Malkin, V., Eds.; Wiley-VCH Verlag: Weinheim, 2004; p 449.
(47) Stewart, A. *Zeolites* **1989**, *9*, 140.
(48) Fyfe, C. A.; O'Brien, J. H.; Strobl, H. *Nature* **1987**, *326*, 281.
(49) Tycko, R.; Dabbagh, G.; Mirau, P. A. *J. Magn. Reson.* **1989**, *85*, 265.
(50) Bak, M.; Rasmussen, J. T.; Nielsen, N. C. *J. Magn. Reson.* **2000**, *147*, 296.
(51) Zaremba, S. *Ann. Mat. Pura. Appl.* **1966**, *73*, 293.
(52) Conroy, H. *J. Chem. Phys.* **1967**, *47*, 5307.
(53) Cheng, V. B.; Suzukawa, J. H. H.; Wolfsberg, M. *J. Chem. Phys.* **1973**, *59*, 3992.

for quantifying the CS tensor was employed, in which the three principal components of the CS tensor, $\delta_{11} \geq \delta_{22} \geq \delta_{33}$, are expressed in terms of the isotropic chemical shift $\delta_{iso} = (\delta_{11} + \delta_{22} + \delta_{33})/3$ which is observed in MAS experiments, the span $\Omega = \delta_{11} - \delta_{33}$ which describes the breadth of the tensor, and the skew $\kappa = (3\delta_{22} - \delta_{iso})/\Omega$ which describes the asymmetry of the tensor. To find the values of Ω and κ giving the best fit to the experimental data, a series of simulations were carried out over a range of values for Ω and κ. Contour plots of χ^2 (sum of the squares of the differences between experimental and simulated data) as a function of Ω and κ were constructed to locate the values of Ω and κ giving the χ^2 minimum, χ^2_{min}. The uncertainties in Ω and κ were estimated from the values of Ω and κ with $\chi^2 = 2\chi^2_{min}$. The fitting procedure and estimation of uncertainties are described in greater detail in the Supporting Information. The displayed frequency axes of the experimental and best-fit simulated quasi-static powder patterns have been scaled by the pulse sequence scaling factor of 0.393. The experimentally measured principal components of the ^{29}Si CS tensors for all samples are summarized in Figure 11 and are provided in table form in the Supporting Information.

Ab initio Hartree−Fock calculations were performed with Gaussian98 (revision A.11.3)[55] using the gauge-including atomic orbital (GIAO) method[56] for NMR chemical shift calculations. The calculations were carried out on clusters of atoms extracted from the crystal structures with the Si site of interest at the core of each cluster and the outer atoms terminated with hydrogen atoms (using O−H or Si−H distances of 0.96 and 1.48 Å, respectively). For the majority of calculations, each central Si atom was surrounded by three coordination spheres with the outer oxygen atoms terminated with hydrogen atoms. In the case of some clusters in which the atoms in the outer coordination spheres close in on one another to form 4-rings, an additional Si atom was included to close the ring along with two additional oxygen atoms and terminating H atoms. This is the same general strategy for extracting clusters from crystal structures employed in previous work.[38,40,41] Unless otherwise mentioned, the calculations employed 6-311G(2df) basis sets for all atoms in the clusters. These assumptions in cluster size and basis set were validated by performing a series of calculations on α-quartz and Sigma-2 [see Figure S2 (Supporting Information) and Figure 9]. To facilitate comparison of calculated and experimental chemical shifts, the calculated shielding tensor values were converted into chemical shift values using α-quartz as a secondary chemical shift standard. The calculated absolute shielding values, σ, were converted to relative chemical shifts, δ, with respect to TMS using

$$\delta^{TMS}(\text{cluster}) = \sigma_{iso}(\alpha\text{-quartz}) + \delta^{TMS}_{iso}(\alpha\text{-quartz}) - \sigma(\text{cluster})$$

where σ_{iso}(α-quartz) and σ(cluster) are calculated using the same basis set and cluster size. The experimentally observed isotropic chemical shift for α-quartz was $\delta^{TMS}_{iso}(\alpha\text{-quartz}) = -107.28$ ppm (see Figure 8). For the cluster extracted from the α-quartz crystal structure[57] with three coordination spheres and using the 6-311G(2df) basis set for all atoms, the calculated absolute isotropic shielding value was $\sigma_{iso}(\alpha\text{-quartz}) = 490.70$ ppm. The calculated principal components of the ^{29}Si shielding tensors for all materials are summarized and compared to the experimental values in Figure 11 and provided in table form in the Supporting Information.

X-ray diffraction measurements on a 0.10 × 0.10 × 0.08 mm^3 single crystal of the same Sigma-2 sample studied by solid-state NMR were performed at room temperature on a Bruker Kappa APEXII CCD diffractometer equipped with Mo Kα radiation (0.71073 Å). In order to obtain accurate coordinates for the framework atoms, a highly redundant (38 107 reflections total, 3062 unique) high-resolution (0.55 Å) data set was collected. As in a previous powder X-ray study,[58] the structure was solved and refined in the tetragonal ($a = 10.2316$, $c = 34.3642$ Å) space group $I4_1/amd$. The 1-aminoadamantane template was disordered over eight overlapped symmetry-related sites. Final residuals were R1 = 0.0271 and wR2 = 0.0740. Further details of the structure determination and a crystallographic information file are provided as Supporting Information.

Results and Discussion

The most accurate way to measure full CS tensors (principal components and orientation) is to collect NMR data on a single crystal. However, in most circumstances, particularly in the case of zeolites, single crystals of suitable dimensions for NMR are exceedingly rare (see ref 59 for an exception). For the vast majority of materials, NMR experiments are limited to powder samples, and the CS tensor information is limited to the principal components. A static NMR spectrum of a powder sample is the most straightforward way to measure the principal components of CS tensors, but only if there is a small number of unique sites and their powder patterns do not significantly overlap. For materials with multiple unique sites and overlapping powder patterns, it is usually necessary to employ MAS in order to resolve the various sites according to their isotropic chemical shifts. If a slow enough spinning frequency is used, the spectrum will consist of spinning sideband patterns that can be analyzed to obtain the anisotropy and asymmetry of the CS tensors.[54]

However, this approach is not amenable to the measurement of ^{29}Si CS tensors for many zeolites since the magnitudes of the ^{29}Si chemical shift anisotropies are small. Slow MAS frequencies are required in order to maintain a sufficient number of spinning sidebands from which to measure the span and skew of the CS tensors. For zeolites with multiple Si sites, it is often difficult to find a suitably slow MAS frequency for which the spinning sidebands and isotropic peaks remain resolved from one another. Consequently, an alternative approach is required.

There are a number of NMR methods available for measuring CS tensors in the situation of a high degree of spectral overlap, most of which involve multipulse and multidimensional NMR pulse sequences and/or specialized hardware. The methods involving moving away from the magic-angle[60−62] and extremely slow magic-angle "turning"[63−65] were not feasible in our laboratory due the specialized nature of the required equipment. Following the approach of Alla et al.,[66] a number of 2D experiments have been developed in which multiple pulses are applied in synchronization with the rotation of the sample in order to reintroduce or "recouple" the chemical shift anisotropy interaction and observe it indirectly in the second dimension. Some of these methods separate the spinning sidebands according to their order,[67−69] while others correlate

(54) Herzfeld, J.; Berger, A. E. *J. Chem. Phys.* **1980**, *73*, 6021.
(55) Frisch, M. J.; et al. *Gaussian 98*, Revision A.11.3; Gaussian, Inc.: Pittsburgh, PA, 2002.
(56) Ditchfield, R. *Mol. Phys.* **1974**, *27*, 789
(57) Levian, L.; Prewitt, C. T.; Weidner, D. J. *Am. Mineral.* **1980**, *65*, 920.
(58) McCusker, L. B. *J. Appl. Crystallogr.* **1988**, *21*, 305.
(59) Terskikh, V. V.; Moudrakovski, I. L.; Du, H.; Ratcliffe, C. I.; Ripmeester, J. A. *J. Am. Chem. Soc.* **2001**, *123*, 10399.
(60) Bax, A.; Szeverenyi, N. M.; Maciel, G. E. *J. Magn. Reson.* **1983**, *55*, 494.
(61) Terao, T.; Fujii, T.; Onodera, T.; Saika, A. *Chem. Phys. Lett.* **1984**, *107*, 145.
(62) Frydman, L.; Chingas, G. C.; Lee, Y. K.; Grandinetti, P. J.; Eastman, M. A.; Barrall, G. A.; Pines, A. *J. Chem. Phys.* **1992**, *97*, 4800.
(63) Gan, Z. *J. Am. Chem. Soc.* **1992**, *114*, 8307.
(64) Hu, J. Z.; Orendt, A. M.; Alderman, D. W.; Pugmire, R. J.; Ye, C.; Grant, D. M. *Solid State Nucl. Magn. Reson.* **1994**, *3*, 181.
(65) Hu, J. Z.; Wang, W.; Liu, F.; Solum, M. S.; Alderman, D. W.; Pugmire, R. J.; Grant, D. M. *J. Magn. Reson. A* **1995**, *113*, 210.
(66) Alla, M. A.; Kundla, E. I.; Lippma, E. T. *JETP Lett.* **1978**, *27*, 194.
(67) De Lacroix, S. F.; Titman, J. J.; Hagemeyer, A.; Spiess, H. W. *J. Magn. Reson.* **1992**, *97*, 435.

scaled spinning sideband patterns to their isotropic shifts.[70−74] Another set of experiments gives 2D spectra in which "quasi-static" powder patterns are correlated to the isotropic peaks.[49,75−78] In these spectra, each of the powder patterns that would be observed in a static NMR experiment is observed (albeit scaled) in the indirect dimension and separated from the other patterns according to the isotropic shifts observed in the direct dimension due to magic-angle spinning.

Since the anisotropies of zeolite ^{29}Si CS tensors are quite small, even at ultrahigh magnetic fields, it is necessary to employ a recoupling pulse sequence that gives undistorted quasi-static powder patterns and both is robust to experimental errors and has a large scaling factor. The four-π-pulse sequence developed by Tycko et al.[49] (Figure 1a) gives undistorted powder patterns with a large scaling factor of 0.393, but suffers from a strong sensitivity to errors in the recoupling pulses. As the simulations in Figure 1c demonstrate, even small errors in the pulses, perhaps due to mis-setting the pulse lengths or the inevitable rf inhomogeneity, will lead to an underestimation of the span of the CS tensor. In order to improve the robustness of the sequence, the 180° recoupling pulses were replaced with 90°−180°−90° composite pulses[79] (see Figure 1b) that are known to compensate for rf errors. As the simulations in Figure 1d demonstrate, the improved robustness of this pulse sequence is quite dramatic, showing little deviation of the expected powder pattern with rf errors as large as 20%. We feel that this pulse sequence is more suitable than the SUPER sequence[77] for measuring zeolite ^{29}Si CS tensors since, like SUPER, it gives undistorted powder patterns and is very robust toward pulse errors, but it has a much larger scaling factor (0.393 compared to 0.155) and does not require shearing of the indirect dimension during processing of the data.

The CSA recoupling experiment was first carried out on the clathrasil Sigma-2, a material that has been found to be ideal for testing and developing ^{29}Si NMR experiments for zeolites. The 2D ^{29}Si anisotropic−isotropic correlation spectrum for Sigma-2 is presented in Figure 2a. Since Sigma-2 has four crystallographically unique Si sites in its structure, four isotropic peaks are observed. The peaks have been previously assigned to the Si sites using a ^{29}Si 2D correlation experiment.[17] Distinct powder patterns are observed for each of these four sites in the 2D CSA recoupling spectrum. The best-fit simulated powder patterns for each site are displayed in Figure 2b, and the χ^2 plots of the difference between the experimental and simulated powder patterns as functions of the span Ω and skew κ are displayed in Figure 2c, from which the best-fit values and their uncertainties were estimated. The CSA recoupling experiment was also performed on the zeolite ZSM-12. As the ^{29}Si MAS spectrum in Figure 3a shows, this material has seven crystallographically unique Si sites, each of which gives a distinct

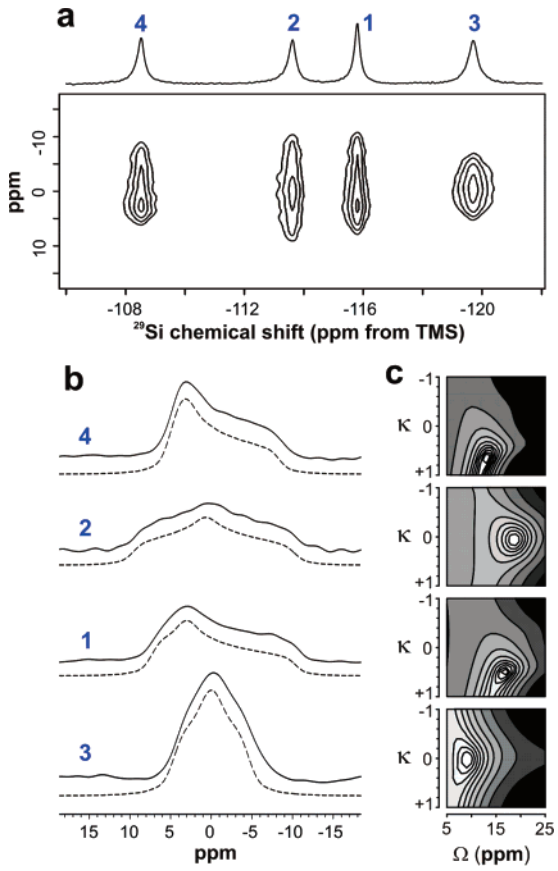

Figure 2. (a) 2D ^{29}Si CSA recoupling spectrum for the clathrasil Sigma-2. The numbering scheme corresponds to the Si sites in the crystal structure of Sigma-2.[58] (b) Experimental (solid lines) and best-fit simulated (dashed lines) quasi-static CSA recoupled line shapes for the indicated Si sites extracted from the 2D spectrum. (c) Contour plots of the quality of fit (χ^2) of simulated to experimental line shapes as functions of span Ω and skew κ (the nth contour level is at $2^{n/2}\chi^2_{min}$). The best-fit values and estimated uncertainties are listed in Table S1 (Suppporting Information) and displayed in Figure 11.

powder pattern with the CSA recoupling experiment (Figure 3b). The peaks have been previously assigned to the Si sites in the crystal structure using a ^{29}Si 2D correlation experiment.[80] The best-fit simulated powder patterns are displayed as dashed lines in Figure 3b.

In order to verify that the ^{29}Si CS tensor values measured in this recoupling experiment are reliable, ^{29}Si MAS NMR spectra were also collected for Sigma-2 and ZSM-12 with slow spinning frequencies such that the CS tensor values could be determined from the spinning sideband patterns. Figure 4 shows the spectrum for Sigma-2 collected at a spinning frequency of 600 Hz, along with the best-fit spectrum and sub-spectra for each of the four Si sites. A slow MAS spectrum for ZSM-12 is presented in Figure S1 in the Supporting Information. In Figure 5 , the span and skew values determined by the two different experiments are plotted against each other. Although the recoupling method tends to slightly underestimate the span of the tensor and gives uncertainties that are typically larger than those determined from the slow MAS spectra, this comparison demonstrates that the recoupling method can reliably measure the principal components of ^{29}Si CS tensors in these materials.

(68) Antzutkin, O. N.; Shekar, S. C.; Levitt, M. H. *J. Magn. Reson. A* **1995**, *115*, 7.
(69) Antzutkin, O. N.; Lee, Y. K.; Levitt, M. H. *J. Magn. Reson.* **1998**, *135*, 144.
(70) Crockford, C.; Geen, H.; Titman, J. J. *Chem. Phys. Lett.* **2001**, *344*, 367.
(71) Elena, B.; Hediger, S.; Emsley, L. *J. Magn. Reson.* **2003**, *160*, 40.
(72) Gullion, T. *J. Magn. Reson.* **1989**, *85*, 614.
(73) Kolbert, A. C.; Griffin, R. G. *Chem. Phys. Lett.* **1990**, *166*, 87.
(74) Orr, R. M.; Duer, M. J.; Ashbrook, S. E. *J. Magn. Reson.* **2005**, *174*, 301.
(75) Bax, A.; Szeverenyi, N. M.; Maciel, G. E. *J. Magn. Reson.* **1983**, *51*, 400.
(76) Chan, J. C. C.; Tycko, R. *J. Chem. Phys.* **2003**, *118*, 8378.
(77) Liu, S. F.; Mao, J. D.; Schmidt-Rohr, K. *J. Magn. Reson.* **2002**, *155*, 15.
(78) Orr, R. M.; Duer, M. J. *J. Magn. Reson.* **2006**, *181*, 1.
(79) Levitt, M. H.; Freeman, R. *J. Magn. Reson.* **1979**, *33*, 473.
(80) Fyfe, C. A.; Feng, Y.; Gies, H.; Grondey, H.; Kokotailo, G. T. *J. Am. Chem. Soc.* **1990**, *112*, 3264.

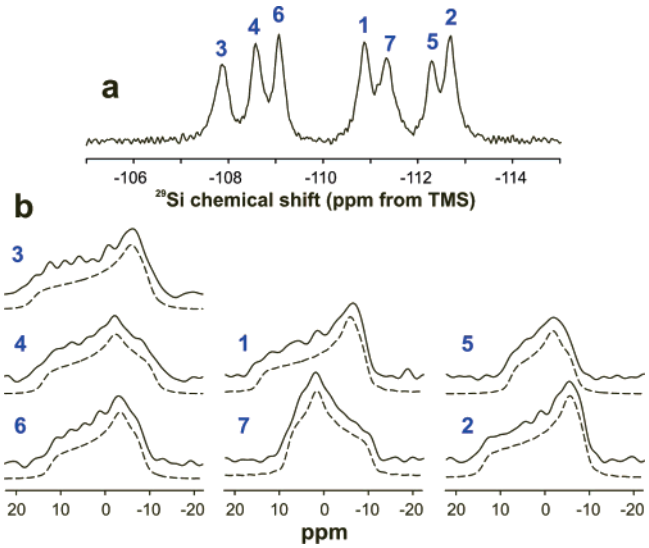

Figure 3. (a) 1D ^{29}Si MAS NMR spectrum of ZSM-12 zeolite (128 scans). The numbering scheme corresponds to the Si sites in the crystal structure of ZSM-12.[10] (b) Experimental (solid lines) and best-fit simulated (dashed lines) quasi-static CSA recoupled line shapes for the indicated Si sites extracted from the 2D spectrum for ZSM-12 (not shown). The best-fit values of Ω and κ and their estimated uncertainties are listed in Table S2 (Supporting Information) and displayed in Figure 11.

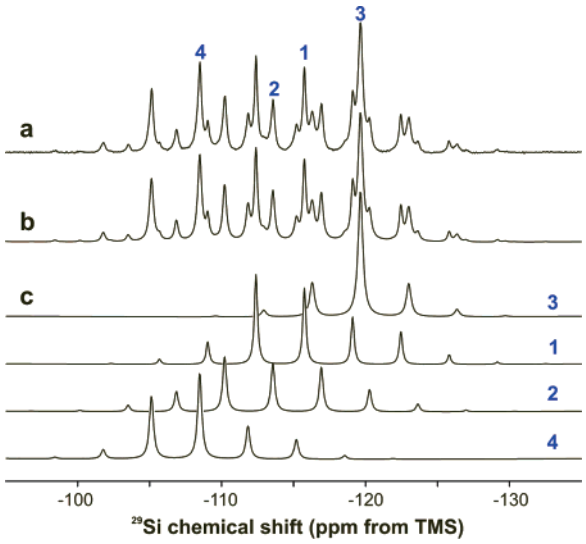

Figure 4. (a) Experimental ^{29}Si CP MAS NMR spectra of Sigma-2 obtained at MAS spinning frequency of 600 Hz (512 scans, 2 s recycle delay). The numbers represent the Si sites and indicate the isotropic shifts. (b) Simulated MAS spectrum composed of (c) individual simulated spinning sideband patterns for each Si site. The best-fit values of Ω and κ and their estimated uncertainties are listed in Table S1 (Supporting Information) and displayed in Figure 11.

With the reliability of the CSA recoupling experiment established, the experiment was applied to a zeolite whose spectral complexity ruled out the possibility of measuring the CS tensors from slow spinning MAS spectra. As the number of Si sites (and isotropic peaks in the ^{29}Si spectra) increases, it becomes increasingly difficult, if not impossible, to find a suitable slow spinning frequency for which the spinning sidebands are resolved and for which there are a sufficient number of spinning sidebands for reliable measurements of the CS tensor values. The monoclinic phase of empty calcined silica-ZSM-5 presents the most difficult case. The ^{29}Si MAS NMR spectrum (Figure 6a) is extremely complicated and crowded due

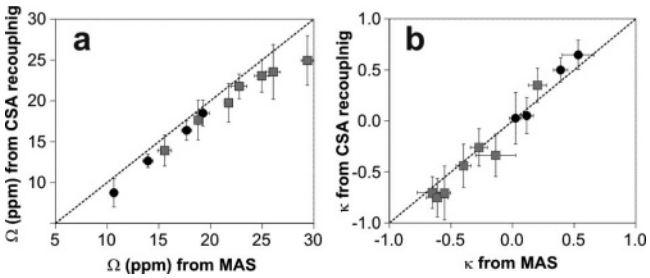

Figure 5. Comparison of (a) the span Ω and (b) the skew κ values determined from the CSA recoupling experiment to those determined by analysis of the spinning sideband patterns in the slow MAS experiments. The black circles and gray squares represent the values obtained for Sigma-2 and ZSM-12, respectively.

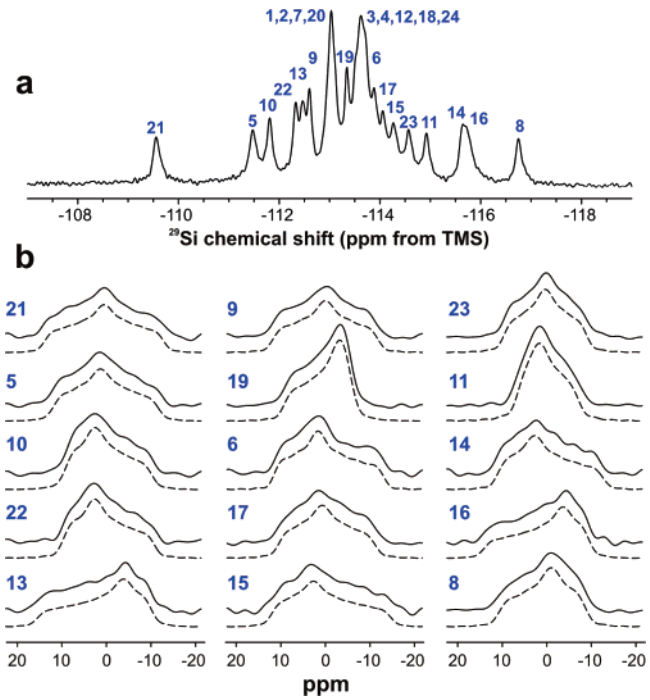

Figure 6. (a) 1D ^{29}Si MAS NMR spectrum of room-temperature monoclinic phase of silica-ZSM-5 zeolite (384 scans). The numbering scheme corresponds to the Si sites in the crystal structure of ZSM-5.[81] (b) Experimental (solid lines) and best-fit simulated (dashed lines) quasi-static CSA recoupled line shapes for the indicated Si sites extracted from the 2D spectrum (not shown). The best-fit values of Ω and κ and their estimated uncertainties are listed in Table S3 (Supporting Information) and displayed in Figure 11.

to the presence of 24 unique Si sites in the crystal structure.[48] The peaks in the ^{29}Si spectrum have been previously assigned to the Si sites in the crystal structure[81] using a ^{29}Si 2D correlation experiment.[82] The 2D CSA recoupling experiment enables the quasi-static powder patterns to be obtained for 15 resolved isotropic peaks in the spectrum (Figure 6b). It is reiterated that these measurements would not be possible with slow MAS experiments due to the high degree of spectral overlap.

For the data presented here for these three zeolite samples, the ^{29}Si CS tensors were found to range in span from about 10 to 30 ppm, while the skew values covered the full range from −1 to +1, with none of the tensors found to be explicitly axially symmetric. This range of CS tensor values must be a reflection

(81) van Koningsveld, H.; Jansen, J. C.; van Bekkum, H. *Zeolites* **1990**, *10*, 235.
(82) Fyfe, C. A.; Grondey, H.; Feng, Y.; Kokotailo, G. T. *J. Am. Chem. Soc.* **1990**, *112*, 8812.

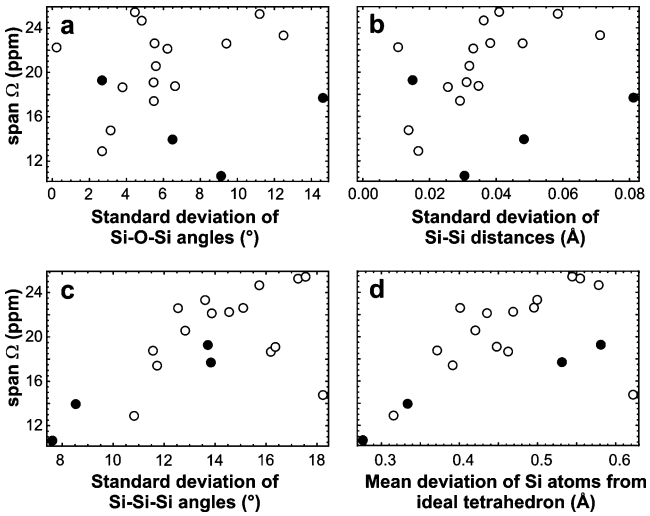

Figure 7. Plots of the span Ω of the ^{29}Si chemical shift tensors for Sigma-2 (filled circles) and silica-ZSM-5 (open circles) against various structural parameters: (a) standard deviation of the four Si−O−Si bond angles around each central Si atom, (b) standard deviation of the Si−Si distances to the four closest Si atoms from each central Si atom, (c) standard deviation of the six Si−Si−Si angles around each central Si atoms, and (d) mean deviation of the neighboring Si atoms from a rotated and scaled ideal tetrahedron centered on each central Si atom (see text).

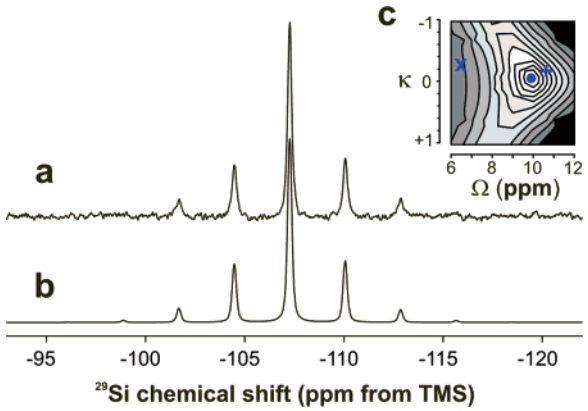

Figure 8. (a) Experimental ^{29}Si MAS NMR spectrum of α-quartz obtained at a magnetic field of 21.1 T and a spinning frequency of 500 Hz. (b) Best-fit simulated spectrum with $\delta_{iso} = -107.28$ ppm, $\Omega = 9.7 \pm 0.5$ ppm, and $\kappa = -0.05 \pm 0.15$. (c) Contour plots of the quality of fit (χ^2) of simulated to experimental spectra as functions of span Ω and skew κ (the nth contour level is at $2^{n/2}\chi^2_{min}$). The filled circle (●) denotes the best-fit values, the plus (+) denotes the *ab initio* calculated values, and the cross (×) denotes the values determined in a single-crystal NMR study at 9.4 T.[18]

of the variety of local structural environments in which the Si atoms can be found. An attempt was made to correlate the anisotropy of the CS tensors to simple structural parameters such as local bond lengths and bond angles. No correlations were found for structural parameters describing the first coordination sphere, such as Si−O bond lengths and O−Si−O bond angles. This is not unsurprising, since the SiO_4 units from which zeolite frameworks are constructed are very close to ideal tetrahedrons.

Since the isotropic ^{29}Si chemical shifts correlate well with parameters derived from the Si−O−Si bond angles, correlations between the span of the ^{29}Si CS tensors and structural parameters involving the second coordination sphere were investigated (see Figure 7). Although the isotropic shifts correlate well with the mean Si−O−Si bond angles and with the mean Si−Si distances, there does not exist a correlation between the span and the standard deviations of these parameters, as shown in Figure 7a,b, respectively. However, weak correlations between the span and structural parameters describing the distortion of the neighboring Si atoms from an ideal tetrahedron do exist. Figure 7c shows that, as the standard deviations of the six Si−Si−Si angles around each central Si increase, the span tends to increase. Similarly, Figure 7d shows that the span tends to increase as the mean deviation of the Si atoms from an ideal tetrahedron increases. (The center of an ideal tetradedron was fixed on the Si atom in question, and this tetrahedron was rotated and scaled in order to minimize the mean deviation of the neighboring Si atoms from the vertices of the ideal tetrahedron.) No correlations between the skew of the ^{29}Si CS tensors and these structural parameters were found (data not shown).

Unfortunately, neither of these correlations is particularly strong, nor could we find any better correlations with other simple structural parameters. These results indicate that the ^{29}Si CS tensors are certainly related to local structure, but that the relationship is clearly not a simple one that can be distilled into a straightforward correlation to one single structural parameter. There are likely to be multiple effects that can only be addressed by performing *ab initio* calculations of the ^{29}Si shielding tensors. For example, the obvious outlying point in the correlation in Figure 7d belongs to Si19 of the silica-ZSM-5 structure, yet the ^{29}Si CS tensor components calculated for this Si site using *ab initio* methods agree very well with the experimental measurements (see below).

Before the results of the *ab initio* calculations are presented and discussed, it is worthwhile to present one more experimental result, the ^{29}Si MAS NMR spectrum of α-quartz collected at 21.1 T. Since α-quartz is used as a reference material for converting the calculated magnetic shielding values in to chemical shift values, it is important to establish that the *ab initio* calculations for α-quartz are in good agreement with experiment. It was also felt that it was important to accurately measure the isotropic shift using the exact same TMS reference sample that was used for all of the zeolite spectra reported in this work. A meaningful test of the accuracy of an *ab initio* calculation is how well it can calculate the span and skew of the ^{29}Si CS tensor. These experimental values were estimated by fitting the spinning sideband profile (Figure 8b) and were found to be $\delta_{iso} = -107.28$ ppm, $\Omega = 9.7 \pm 0.5$ ppm, and $\kappa = -0.05 \pm 0.15$. The uncertainties were estimated from the χ^2 contour plot shown in Figure 8c. These values are compared in Figure 8c to the ^{29}Si CS tensor values ($\Omega = 6.5$ ppm and $\kappa = -0.35$) determined in a single-crystal NMR study[18] performed on a lower field instrument (9.4 T). In general, single-crystal NMR data tend to be more informative and reliable than NMR data collected on polycrystalline powders. However, in this case, the fact that the spectrum was collected at a much higher magnetic field strength and that the *ab initio* calculations (see below) are in much better agreement suggest that the present experimental results are more reliable than the older single-crystal NMR study.

In order to determine the cluster size and basis sets required to accurately calculate the ^{29}Si shielding tensor components from first principles, a series of calculations were first carried out for α-quartz, using the atomic coordinates determined in a reliable single-crystal XRD study.[57] The results of these calculations are presented in Figure S2 in the Supporting

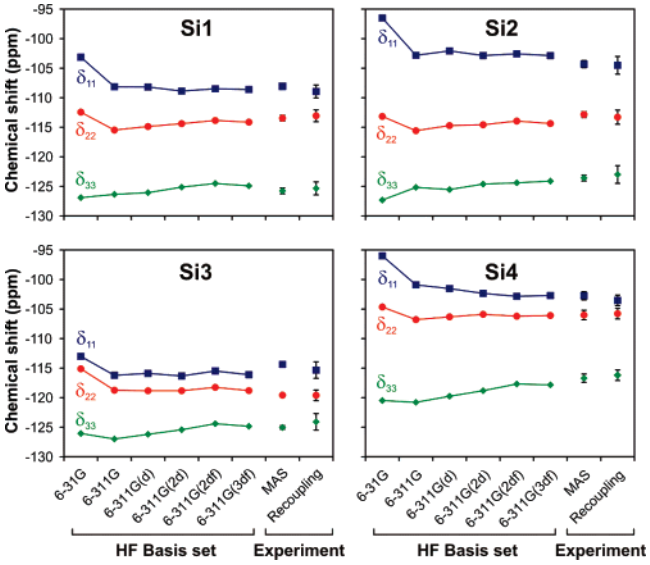

Figure 9. Comparison of the *ab initio* calculated principal components of the ^{29}Si chemical shift tensors for Sigma-2 as functions of basis set to the experimental values. The *ab initio* calculations were performed using atomic coordinates from the single-crystal XRD structure of Sigma-2. The calculated magnetic shielding values were converted to chemical shifts using the isotropic shielding value for α-quartz calculated with the same basis set.

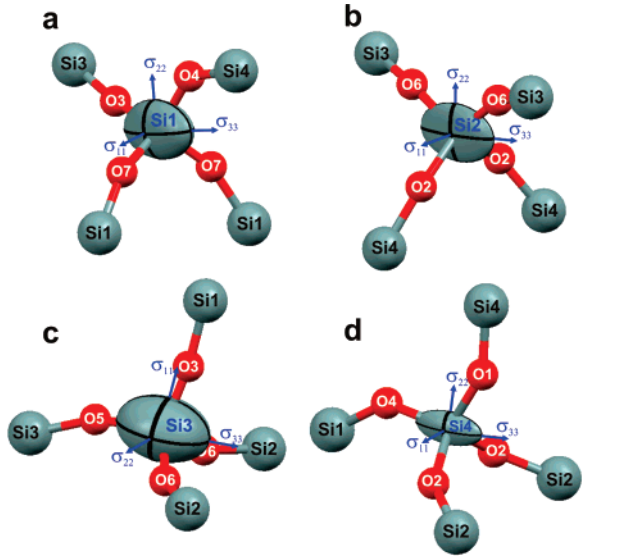

Figure 10. Local structural geometry and ellipsoid representations of the *ab initio* calculated ^{29}Si shielding tensors for the Si sites in Sigma-2: (a) Si1, (b) Si2, (c) Si3, and (d) Si4. In order to emphasize the shielding tensor asymmetry in the ellipsoid representations, a constant value of 480 ppm (corresponding to −96.58 ppm on the ^{29}Si chemical shift scale referenced to TMS) was subtracted from each principal component of the shielding tensor, such that the magnitudes of the ellipsoid principal axes are proportional to $\sigma_{11} - 480$, $\sigma_{22} - 480$, and $\sigma_{33} - 480$ ppm. Note that the size of an ellipsoid is a reflection of the magnitude of the isotropic shielding, while the *distortion* of an ellipsoid from a sphere reflects the anisotropy of the shielding tensor.

Information. Suitable convergence in the shielding parameters was achieved with the 6-311G(2df) basis set and for clusters with three coordination spheres. Therefore, unless otherwise specified, all of the calculations described below employed clusters with three coordination spheres about the central Si atom and the 6-311G(2df) basis set for all atoms. The *ab initio* calculation for α-quartz using this cluster size and basis set yields values of $\Omega = 10.7$ ppm and $\kappa = -0.22$. This good agreement with the experimental values (see Figure 8c) is a promising indication that it should be possible to accurately calculate the zeolite ^{29}Si shielding tensors as well.

Figure 9 presents the results of a series of calculations of the ^{29}Si shielding tensor components for Sigma-2. In order to ensure that the highest possible quality structural data were used, the crystal structure of Sigma-2, previously determined from synchrotron powder XRD data,[58] was redetermined from single-crystal XRD data. The details of this structure determination are provided in the Supporting Information. The calculation results presented in Figure 9 provide further support for the choice of basis set and cluster size. The calculated values converge at the 6-311G(2df) level and are in excellent agreement with the experimentally determined values. It should be noted that any potential contributions of the template molecules in Sigma-2 to the shielding interaction have been neglected. *Ab initio* calculations were also performed using the Sigma-2 structure determined from synchrotron powder XRD data. These calculated ^{29}Si shielding tensors were found to be in poorer agreement with experimental values than those calculated from the single-crystal XRD structure (see below).

The relationships of the ^{29}Si shielding tensors to the local structure around each Si atom in Sigma-2 are depicted in Figure 10. Each of the Si atoms lies on a special crystallographic position, and this local symmetry is reflected in the orientations of the shielding tensors. Si1 lies on a mirror plane along with Si3, Si4, O3, and O4 (see Figure 10a). The least shielded tensor component, σ_{11}, is perpendicular to this plane, while σ_{22} and σ_{33} lie in the plane, with the angle between the Si1−O4 vector and the σ_{33} direction being 45°. Si3 also lies on a mirror place along with Si1, another Si3, O3, and O5 (see Figure 10c). In this case, the least shielded tensor component, σ_{11}, is in this plane along with the most shielded component, σ_{33}, while σ_{22} is perpendicular to the plane. The angle between the Si3−O3 vector and the σ_{33} direction is 78°. Si4 lies on a mirror place along with another Si4, Si1, O1, and O4 (see Figure 10d). The least shielded tensor component, σ_{11}, is perpendicular to this plane, while σ_{22} and σ_{33} lie in the plane, with the angle between the Si4−O1 vector and the σ_{33} direction being 60°. Si2 represents a different environment, as it lies on a two-fold rotation axis (see Figure 10b). Here, σ_{22} is parallel to this rotation axis, while σ_{11} is perpendicular to the plane defined by O6, Si2, and O6 but parallel to the O2−O2 vector, and σ_{22} is perpendicular to the plane defined by O2, Si2, and O2 but parallel to the O6−O6 vector. Again, it is clear that there is a strong relationship between the ^{29}Si shielding tensors and the local structure around the Si atoms. However, it is not straightforward to predict the orientations and principal components of the ^{29}Si shielding tensors directly from the local structural geometry without resorting to *ab initio* calculations.

The results of all of the *ab initio* ^{29}Si shielding tensor calculations for α-quartz, Sigma-2, ZSM-12, and ZSM-5 are presented in Figure 11, where these results are also compared to all of the experimental data presented above. In general, the calculated and experimental values are in very good agreement, with the exception of the ZSM-12 results. The plot for Si2 of ZSM-12 (Figure 11c) illustrates an important point about measuring and calculating the ^{29}Si CS tensor components. The experimental and calculated principal components are very different, yet the isotropic values are in excellent agreement. If

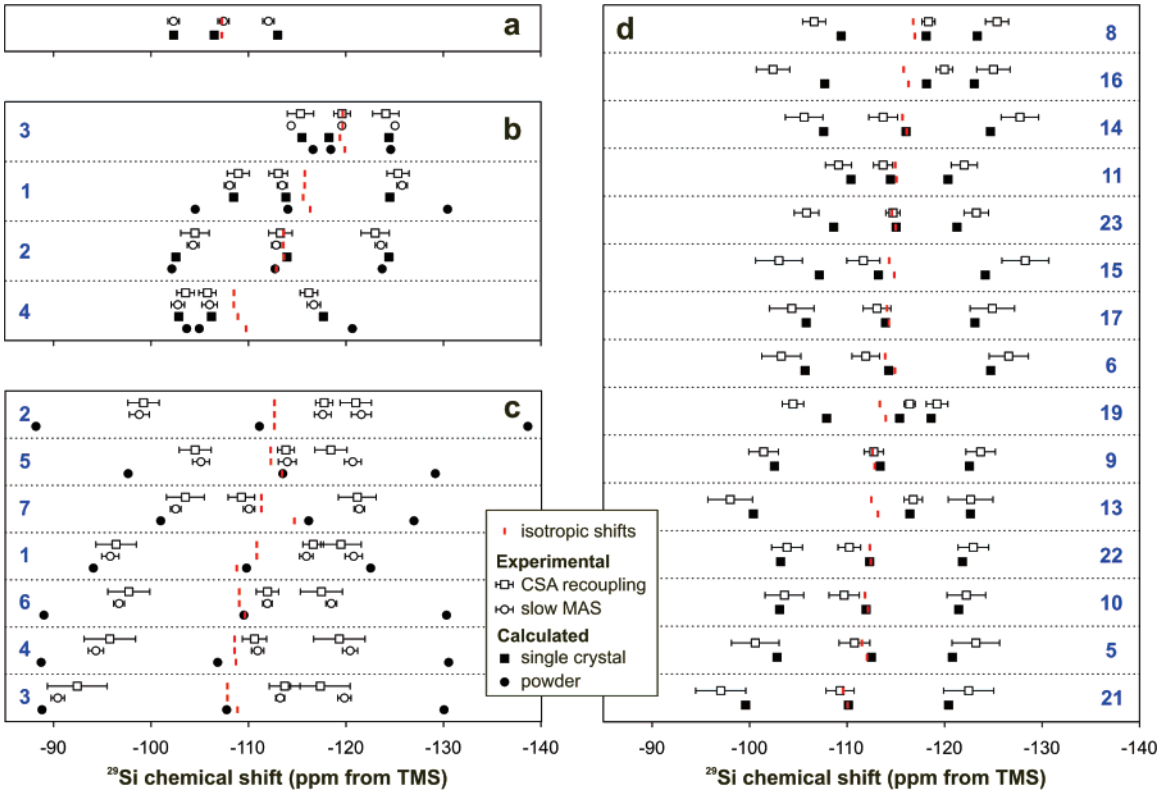

Figure 11. Comparison of the experimental (open symbols) and *ab initio* calculated (filled symbols) principal components of ^{29}Si chemical shift tensors for (a) α-quartz, (b) Sigma-2, (c) ZSM-12, and (d) the monoclinic phase of ZSM-5. The open squares and circles represent experimental data from the 2D CSA recoupling and slow MAS experiments, respectively, while the filled squares and circles represent the calculated values using crystal structures determined from single-crystal and powder XRD data, respectively. The red lines represent the ^{29}Si isotropic chemical shifts in each case. The data are ordered according experimental ^{29}Si isotropic chemical shifts. All numerical values are provided in the Supporting Information.

only isotropic values were being evaluated, one could conclude that the experiment and calculations are in good agreement. However, by evaluating the tensor components, it becomes very clear that something is wrong.

It is interesting to note that the largest deviations occur for calculations that use atomic coordinates derived from powder XRD data. Figure 12 presents a clearer comparison of the quality of agreement between the calculated and experimental chemical shift parameters for calculations carried out using atomic coordinates determined from powder XRD data and those determined in a single-crystal XRD study. The calculations for Sigma-2 (Figure 12a,b) demonstrate that, as the quality of the crystal structure improves from powder[58] to single-crystal structures, the agreement between the calculated and experimental values improves quite significantly. The root-mean-square (rms) deviation between the calculated and experimental values in Figure 12a for the powder XRD structure of Sigma-2 is 2.5 ppm, while it improves to 1.0 ppm for the single-crystal XRD structure (Figure 12b). The uncertainties in the atomic positions in the single-crystal structure are more than an order of magnitude smaller than those in the powder structure. It is significant that, as the crystal structure becomes more precise, the calculated ^{29}Si shielding tensor components become more accurate. The mean differences in the atomic positions between the powder and single-crystal structures are only 0.008 and 0.016 Å for the Si and O atoms, respectively, indicating that the ^{29}Si magnetic shielding interaction is extremely sensitive to the local structural geometry.

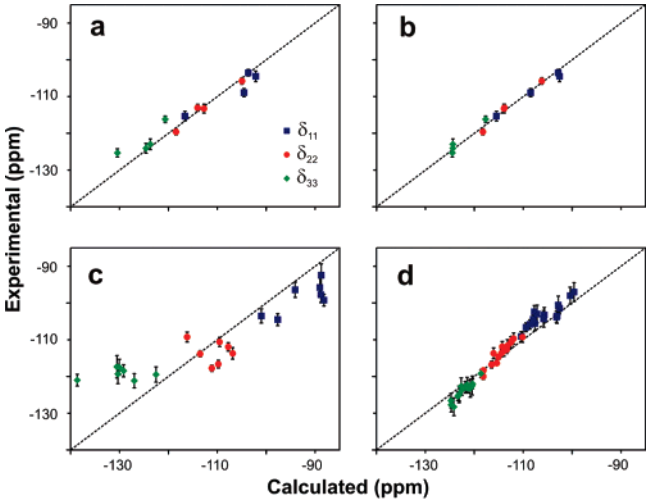

Figure 12. Quality of agreement between experiment and *ab initio* calculations of the principal components of the ^{29}Si chemical shift tensors for (a) Sigma-2 using the synchrotron powder XRD structure,[58] (b) Sigma-2 using the single-crystal XRD structure, (c) ZSM-12 crystal structure determined from synchrotron powder XRD data,[10] and (d) monoclinic ZSM-5 structure determined from single-crystal XRD data.[81] The experimental data are those determined in CSA recoupling experiments. The dashed lines correspond to a perfect agreement between experimental and calculated values.

Figure 12c clearly shows that the calculated ^{29}Si shielding tensor components for ZSM-12 are in very poor agreement with the experimental values (rms = 8.3 ppm). This suggests that the crystal structure for ZSM-12 is probably of quite low quality,

which is not unsurprising since it was determined from powder XRD data.[10] On the contrary, for ZSM-5, whose crystal structure was determined from single-crystal XRD,[81] the quality of agreement between calculated and experimental values is much better. The good agreement for ZSM-5 (rms = 2.1 ppm) is particularly satisfying, as it is one of the most complicated zeolite structures, giving one of the most complicated ^{29}Si NMR spectra, and all of the accessible ^{29}Si CS tensors have been reproduced very well in these calculations. Again, these results indicate that the ^{29}Si chemical shifts are very sensitive to the local structure and that, for *ab initio* calculations of NMR parameters in general, great care must be taken to ensure that the highest possible quality crystal structures are used in order to accurately reproduce experimental data.

The excellent agreement between the experiments and calculations indicates that Hartree−Fock *ab initio* calculations on cluster models extracted from the highest quality crystal structures are certainly sufficient for calculating zeolite ^{29}Si shielding tensors. It should be noted that there have been tremendous advances in the development of periodic DFT methods, such as the gauge-including projector augmented wave (GIPAW) method,[83] that enable calculations of NMR parameters taking into account the periodicity of the crystal structure rather than having to approximate the crystal structure with a suitably large cluster "molecule". This method has recently been applied to the calculation of ^{29}Si and ^{17}O isotropic chemical shifts and ^{17}O quadrupolar parameters for a number of silica polymorphs, including α-quartz and the zeolites ferrierite and faujasite.[45] It would be interesting to compare the accuracy of ^{29}Si shielding tensors calculated by periodic DFT methods and those calculated using a cluster approximation. Because the ^{29}Si shielding tensors seem to be primarily determined by the local structural geometry, which can be adequately accounted for in clusters containing three coordination spheres around a central Si atom, it is not necessarily the case that periodic DFT calculations would give improved results. Furthermore, one of the advantages of using a cluster approximation is that the calculations can be performed on a very complex structure like ZSM-5 by breaking down the crystal structure into a number of clusters, whereas the ZSM-5 structure (with 288 atoms in the unit cell) is probably beyond the present capabilities of periodic DFT calculations. Nonetheless, periodic DFT calculation of zeolite ^{29}Si shielding tensors certainly remains a worthwhile future endeavor in order to fully understand the capabilities and limitations of the various *ab initio* calculation methods.

Conclusions

The principal components of zeolite ^{29}Si magnetic shielding tensors have been accurately measured *and* calculated for the first time. Difficulties in observing the small anisotropies of the ^{29}Si shielding interactions due to Si atoms in near-tetrahedral geometries have been overcome by performing the experiments at an ultrahigh magnetic field of 21.1 T. The spectral complexity which often rules out the application of straightforward one-dimensional slow MAS experiments for measuring CS tensors, most notably in the ^{29}Si spectrum of silica-ZSM-5, has been overcome by employing a robust 2D CSA recoupling pulse sequence. The measured ^{29}Si CS tensors exhibit a surprisingly large range of anisotropies and asymmetries, suggesting that they contain a great deal of information about the local structures around the Si atoms. Although a strong empirical relationship between the CS tensors and simple structural parameters could not be established, the principal components of ^{29}Si shielding tensors in zeolites were accurately calculated with Hartree−Fock *ab initio* calculations on clusters derived from the crystal structures. Although previous work has demonstrated that isotropic values for zeolites can be accurately calculated, this is the first report in which the principal components of the ^{29}Si shielding tensors have been calculated and compared with experimental data. The comparison of the calculations from various crystal structures indicates that the accuracy of the calculations is strongly dependent on the quality of the crystal structure used in the calculation, indicating that the ^{29}Si chemical shift tensors have an exquisite sensitivity to the local structures around the Si atoms.

Work is presently underway on incorporating ^{29}Si CS tensor data and *ab initio* calculations of ^{29}Si shielding tensors into the "NMR crystallography" of zeolites and related materials. It has been previously demonstrated that it is possible to *solve* zeolite crystal structures from ^{29}Si double-quantum NMR experiments.[1] However, the positions of the bridging oxygen atoms remain unknown in these structures, although to a first approximation it can be assumed that they fall somewhere between connected Si atoms. It is anticipated that the complete structures, starting from the Si positions determined by ^{29}Si double-quantum experiments and placing O atoms between Si atoms, could be *refined* to highly accurate structures by adjusting the atomic coordinates to minimize the differences between the experimental and calculated components of the ^{29}Si CS tensors. By having experimental measurements of the three principal components of each ^{29}Si CS tensor, the number of observations is tripled compared to using only the isotropic ^{29}Si chemical shifts. Such a structure refinement technique could also be applied, for example, to the structure of ZSM-12, which shows poor agreement between calculated and experimental ^{29}Si chemical shifts, in order to obtain a more accurate crystal structure than the existing one that is based on synchrotron powder XRD data. Furthermore, with the availability of experimental tools for measuring ^{29}Si CS tensors and the ability to accurately reproduce these values with *ab initio* calculations described here, it is anticipated that this strategy will be important in structural studies of materials for which diffraction experiments provide very limited information, such as disordered layered silicates or silicate glasses.

Acknowledgment. Access to the 900 MHz NMR spectrometer was provided by the National Ultrahigh Field NMR Facility for Solids (Ottawa, Canada), a national research facility funded by the Canada Foundation for Innovation, the Natural Sciences and Engineering Research Council of Canada, the Ontario Innovation Trust, Recherche Québec, the National Research Council Canada, and Bruker BioSpin and managed by the University of Ottawa (www.nmr900.ca). We thank Prof. Colin Fyfe for providing the zeolite samples, Victor Terskikh and Shane Pawsey for assistance in setting up the solid-state NMR experiments, and Stephen Lang, Saman Alavi, and Serguei

(83) Pickard, C. J.; Mauri, F. *Phys. Rev. B* **2001**, *63*, 245101.

Patchkovskii for assistance in setting up the *ab initio* calculations.

Supporting Information Available: Additional details about the experimental conditions and fitting procedures, additional figures, tables of experimental and calculated principal components of ^{29}Si CS tensors, details of the Sigma-2 structure determination from single-crystal XRD data, including a crystallographic information file (CIF), and complete ref 55. This material is available free of charge via the Internet at http://pubs.acs.org.

JA077430A